Specific heat and structure factor in the square ANNNI model by Monte Carlo simulation

E. Rastelli,* S. Regina, and A. Tassi
Dipartimento di Fisica dell'Università, Parco Area delle Scienze 7/A, 43100 Parma, Italy
(Received 4 December 2009; revised manuscript received 15 February 2010; published 25 March 2010)

The axial (or anisotropic) next-nearest-neighbor Ising (ANNNI) model has been widely investigated: exact solution exists in one dimension; analytic and numerical treatments in two, and three dimensions suggest a rich phase diagram. Some controversial results obtained especially by Monte Carlo (MC) simulations are discussed. We conclude that in the region of weak competition ($\kappa=-J_2/J_1<1/2$) the size scaling analysis is the same as that obtained in the nearest-neighbor (NN) Ising model. For $\kappa>1/2$ we find a series of very sharp peaks in the specific heat due to the discreteness of the lattice. The structure factor supports and explains the existence of the specific heat peaks. Very long simulations have been performed (10^7 and 10^8 MC steps per spin) because the relaxation time is huge for such a frustrated system. A careful comparison of MC simulations for different lattice sizes suggests that the Kosterlitz-Thouless phase is present for all $\kappa>1/2$.

DOI: 10.1103/PhysRevB.81.094425 PACS number(s): 75.10.Hk, 75.40.Cx, 75.40.Mg

I. INTRODUCTION

It is well known that competition can introduce dramatic effects in spin lattices even though only short-range interactions are present. The axial (or anisotropic) next-nearest-neighbor Ising (ANNNI) model[1] is a famous example of nonsimple spin configurations produced by simple interactions. The frustration is introduced only in one direction (axial direction) where the next-nearest-neighbor (antiferromagentic) interaction $J_2<0$ competes with the nearest-neighbor (ferromagnetic) one $J_1>0$. A ferromagnetic interaction $J_0>0$ between nearest-neighbor spins is assumed within the lines [two-dimensional (2D) model] or within the planes [three-dimensional (3D) model] perpendicular to the axial direction. An exact solution exists only for the one-dimensional model where no long-range order is found at any nonzero temperature. For $T=0$ one has a ferromagnetic ground state for $\kappa=-J_2/J_1<1/2$ and a $\langle 2\rangle$ phase or antiphase ground state where couples of spins up and down alternate for $\kappa>1/2$. At the point $\kappa=1/2$ and $T=0$ (multiphase point) the ground state is disordered and the entropy per spin is finite.[1] The "disorder line"[2]

$$\kappa=\frac{k_BT}{2J_1}\ln\left[\cosh\left(\frac{J_1}{k_BT}\right)\right] \tag{1}$$

springing from the multiphase point divides the (κ,T) plane in two regions: in the region on the left side of the disorder line the correlation function decays exponentially with the distance between the spins $\langle s_0s_n\rangle\sim\exp(-n/\xi)$ with a correlation length ξ decreasing with increasing temperature; in the region on the right of the disorder line the correlation function is no longer monotonic: indeed $\langle s_0s_n\rangle\sim\exp(-n/\xi)\cos(qn)$ where the wave vector q is a continuous function of κ and T given by

$$q(\kappa,T)=\arccos\left(\frac{\sinh\frac{J_1}{k_BT}}{\sqrt{\exp\frac{4\kappa J_1}{k_BT}-1}}\right). \tag{2}$$

For $T=0$ and $\kappa>1/2$ one has $\xi\to\infty$ and $q=\pi/2$ ($\langle 2\rangle$ phase or antiphase). The staggered susceptibility (proportional to the finite Fourier transform of the correlation function)

$$\frac{k_BT\chi(q)}{\mu^2L}=\sum_n\langle s_0s_n\rangle e^{iqn} \tag{3}$$

shows a two-peak structure around the commensurate wave vectors $q=\pi/2$ and $3\pi/2$ at low temperature. These peaks reduce to δ-like peaks in the limit $T\to0$. Increasing temperature they broaden and move from commensurate to incommensurate values of the wave vectors: $q<\pi/2$ and $q>3\pi/2$, respectively.

No exact solutions exist in two and three dimensions even though many features of the phase diagram are well established on the basis of analytic and numerical results. The phase diagram is divided in four regions:[1] (i) ferromagnetic (F) region for $\kappa<1/2$ and $T<T_f(\kappa)$; (ii) antiphase $\langle 2\rangle$ (commensurate) region consisting of two rows (2D) or two planes (3D) of parallel spins alternating with two rows or two planes of opposite spins for $\kappa>1/2$ and $T<T_a(\kappa)$; and (iii) an incommensurate (IC) phase (possibly of Kosterlitz-Thouless (KT) type in two dimensions) where the wave vector q characterizing the oscillating correlation functions is directed along the axial direction and it is expected to change with temperature and κ: this phase is restricted to a region between the ordered $\langle 2\rangle$ phase and the paramagnetic (P) phase. In the three-dimensional model a Lifshitz point is expected on the F-P transition line[1] whereas it is missing in two dimensions.[3] Another Lifshitz point could occur on the $\langle 2\rangle$-IC transition line in two or three dimensions.[4] Renormalization-group calculations or Monte Carlo (MC) simulations have not been able to solve this puzzle. Other questions remain unsolved: (i) the nature of the F-P transition for $\kappa<1/2$. Calculations performed using the transfer matrix method[5] were not able to clarify whether the F-P transition falls in the universality class of the pure NN Ising model or not even though a first-order transition is predicted[5] as κ goes to 1/2 (the multiphase point). In our work we give results that support the interpretation of Ref. 5 according to which the ANNNI model has always an Ising-type behavior for any $\kappa<1/2$.

(ii) The free fermion approximation[3] (FFA) supports a specific heat that diverges as a power law with critical exponent $\alpha=1/2$ approaching T_f or T_a from the disordered phase. We are able to rule out this behavior for $\kappa<1/2$ where the F-P transition is found to be of Ising type with $\alpha=0$ (logarithmic divergence) and we are led to believe into a discontinuous change in the specific heat instead of a divergence at the $\langle 2\rangle$-IC transition.

(iii) In any case a puzzle is entered by the specific-heat divergence at the $\langle 2\rangle$-IC transition obtained by the FFA.[3] Indeed, since the IC phase is expected to be a KT phase and the specific heat at the conventional order-KT transition is expected to have no singularity, the divergence obtained from the FFA suggests that the IC phase is at least a *sui generis* KT phase.

(iv) Finally, the existence of a Lifshitz point for $\kappa>1/2$ on the $\langle 2\rangle$-IC transition line it is an open question. If the Lifshitz point exists the IC phase disappears at $\kappa=\kappa_L$ and for $\kappa>\kappa_L$ a $\langle 2\rangle$-P phase transition occurs. This transition, however, is characterized by a nonsingular specific heat for $T\rightarrow T_a^-$ and a singular specific heat for $T\rightarrow T_a^+$. By a finite-size scaling we check that κ_L increases with L indicating the persistence of the IC phase for any $\kappa>1/2$.

In this paper we focus on the open questions listed above performing very long MC runs of 10^7 and 10^8 MC steps per spin (MCS) in order to evaluate internal energy, specific heat, and structure factor with the aim of enlighting the nature of the phase transitions. We find that the F-P phase transition for $\kappa<1/2$ is consistent with the universality class of the pure NN Ising model. We have investigated the specific-heat behavior for $\kappa>1/2$ in order to get reliable information on the nature of the IC phase pointed out as modulated or incommensurate phase.[1] The IC phase is believed to be a KT phase on the basis of a not rigorous but sound argument.[6] We find that the $\langle 2\rangle$ phase is driven in the IC phase by the onset of four domain walls consisting of three rows of parallel spins named "three-walls" domains.[1] Increasing temperature eight, twelve, etc., three-walls domains may be recognized in the snapshots and detected by the structure factor, the maximum of which corresponds to a wave-vector spanning all "incommensurate" wave vectors $q=2\pi n/L$ (with $n=L/4,L/4-1,\ldots$, where L is the lattice side of the $L\times L$ lattice) as far as the IC-P phase transition is reached. Monte Carlo simulations for $L=24,48,96$ seem to point out the presence of a Lifshitz point on the $\langle 2\rangle$-P phase boundary. However, we find that κ_L is roughly a linear function of L so that we conclude that the IC phase survives for all $\kappa>1/2$.

II. MONTE CARLO SIMULATIONS

We assume the following Hamiltonian:

$$\mathcal{H}=-J\sum_{i,j}s_{i,j}(s_{i+1,j}+s_{i,j+1}-\kappa s_{i,j+2}), \tag{4}$$

where $s_{i,j}=\pm 1$ is the spin at site (i,j) of a square lattice; $J(=J_0=J_1)>0$ is the NN ferromagnetic interaction and $\kappa=-J_2/J>0$ is the ratio between the NNN antiferromagnetic interaction along the axial direction and the NN ferromagnetic one. This choice is widely adopted in literature, however a slightly different choice is done in Ref. 1 where J_0 is kept constant while $J_1=(1-\alpha)J_0$ and $J_2=-\alpha J_0$ are functions of the parameter α related to κ by the equation $\kappa=\alpha/(1-\alpha)$. Both choices lead to the same limit for $\alpha=0$ ($\kappa=0$) where the ANNNI model reduces to the pure NN Ising model. On the contrary the different choices lead to different limits for $\alpha=1$ ($\kappa\rightarrow\infty$): the parametrization of Ref. 1 leads to a system of two compenetrated decoupled Ising lattices for which the exact solution exists while our parametrization leads to a model in which the intrachain interaction $-\kappa J$ is very strong with respect to the interchain coupling J mocking a rectangular NN Ising model[7] in the limit $\kappa\rightarrow\infty$ so that one expects that k_BT_c/J diverges as $2\kappa/\ln\kappa$.

Monte Carlo simulations are performed on square lattices of size $L=24,48,96$ with periodic boundary conditions. The most of the data points are obtained from runs of 10^7 MCS; far away from the transition region runs of 10^5 MCS were performed. In any case we checked that the difference between the results for 10^5 and 10^7 MCS is within 1%. The temperature is raised by $k_B\Delta T/J=0.01$ taking as initial configuration the last configuration of the previous temperature and disregarding 10^4 MCS for thermalization. We started from the low-temperature configuration where the ground state is known exactly and we performed up to four independent runs. Except for some restricted temperature regions about the phase transition for $\kappa>1/2$, the error bar is within the extension of the symbol of the data points. For $\kappa=0.6$ we have performed either simulations of 10^7 MCS with a scan in temperature of $k_B\Delta T/J=0.001$ or very long simulations of 10^8 MCS (more than one day of cpu for a lattice with $L=96$) for selected temperatures in order to check the reliability of the location and of the height of the specific-heat peaks. Notice that the thermodynamic quantities are obtained averaging over 10^4 configurations that is taking one configuration every 10^3-10^4 MCS so that any correlation between the selected configurations is prevented.

For $0<\kappa<1/2$ the ANNNI model is consistent with the behavior of a pure NN Ising model. In particular, the specific heat for a lattice of $L\times L$ spins

$$C=C_L/(L^2k_B)=\frac{\langle\mathcal{H}^2\rangle-\langle\mathcal{H}\rangle^2}{(Lk_BT)^2} \tag{5}$$

shows a maximum at $T_{\max}$ that scales with L according to the law[8]

$$C_{\max}=A_0(\kappa)\ln L+B(\kappa,\xi) \tag{6}$$

extrapolated from the pure NN Ising model ($\kappa=0$) on a finite lattice $M\times L$ with $\xi=M/L$. Analogously the temperature of the maximum $T_{\max}$ is assumed to be

$$T_{\max}=T_c(\kappa)\left[1-\frac{a(\kappa,\xi)}{L}\right]. \tag{7}$$

Ferdinand and Fisher[8] find that $a(0,\xi)$ is negative for $0.32<\xi<3.14$ and positive otherwise implying that the critical temperature is overstimated for "square" lattices ($\xi=1$) and understimated for "rectangular" lattices. In particular, for a lattice $L\times L$ Ferdinand and Fisher[8] find $A_0(0)=0.49454$, $B(0,1)=0.20136$, and $a(0,1)=-0.36029$.

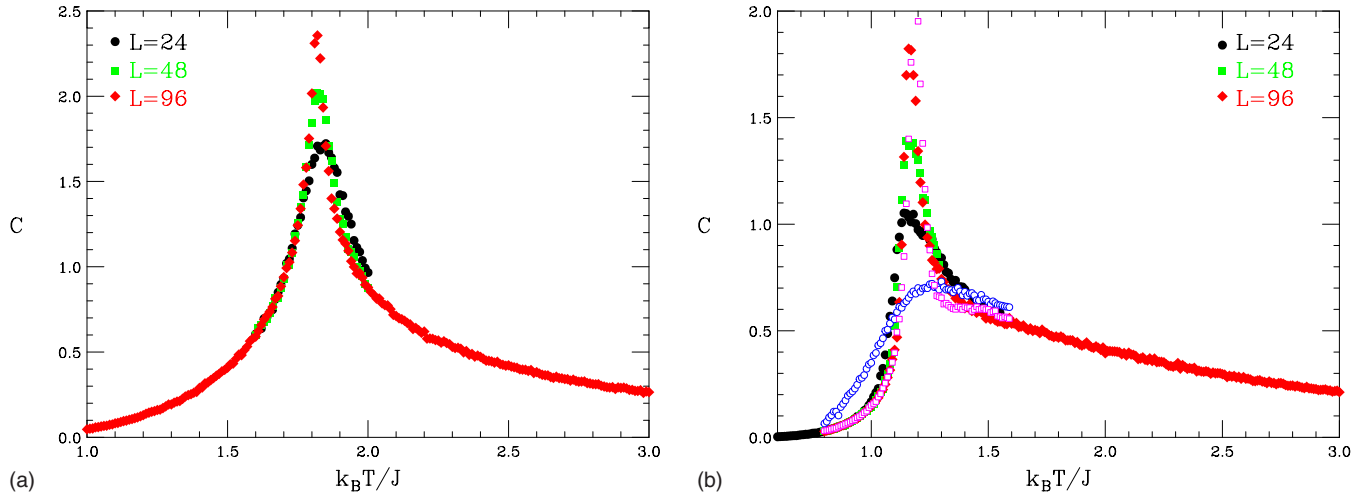

FIG. 1. (Color online) Specific heat vs temperature for (a) $\kappa=0.2$ and for (b) $\kappa=0.4$ obtained from a simulation of 10^7 MCS for lattices of side $L=24$ (full circles), $L=48$ (green squares), and $L=96$ (red diamonds). The (blue) open circles refer to a lattice 12×96 and the (magenta) open squares refer to a lattice 96×12.

For $\kappa\neq0$ no exact result exists: as shown in Fig. 1, however, the specific heat shows a maximum that scales with L in a way quite similar to the case of NN Ising model. For $\kappa=0.2$ and $\kappa=0.4$ we find that Eq. (6) is satisfied assuming $A_0(0.2)=0.47\pm0.01$, $B(0.2,1)=0.21\pm0.05$, and $A_0(0.4)=0.56\pm0.04$ and $B(0.4,1)=-0.73\pm0.15$, respectively.

Our Fig. 1 compares favorably with Fig. 4 of Selke[9] where the specific heat for a rectangular lattice 176×10 ($\xi=17.6$) and several $\alpha=\kappa/(1+\kappa)$ is given. For $\alpha=0$ (NN Ising model) a maximum in the specific heat is found at a temperature $T_{\max}$ lower than the exact critical temperature $k_BT_c/J=2.26919$ in agreement with Eq. (7). Notice that the height of the specific-heat peak is about 1.4, lower than the peak obtained for a 16×16 lattice (see Fig. 1 of Ferdinand and Fisher[8]). The peak of the specific heat for $\alpha=0.15$ (Fig. 4 of Selke[9]) corresponding to $\kappa\simeq0.2$ occurs at a temperature in good agreement with that of our Fig. 1(a). Also in this case the height of the peak ($\simeq1.2$) for the rectangular lattice is lower than that obtained for our smallest square lattice ($\simeq1.7$ for a lattice 24×24).

In Fig. 1(b) the specific heat for $\kappa=0.4$ is shown for several lattice sizes. A one-peak structure very similar to the case $\kappa=0.2$ is clearly seen. The temperature of the maximum increases with L so that the sign of a in Eq. (7) is now positive. In a rectangular lattice with $\xi=17.6$ a (spurious) two-peak structure is found; the one-peak structure is recovered only when the ratio ξ decreases as shown clearly in Fig. 18 of Ref. 9. In order to check a possible power-law temperature dependence of the specific heat about T_c as suggested by the FFA (Ref. 3) or by a finite-size scaling of the transfer-matrix calculation[5] we tried to fit our data with a function $C_{\max}\simeq AL^{\alpha/\nu}$ finding $\alpha/\nu=0.397\pm0.005$ and $A=0.298\pm0.004$ in agreement with the transfer matrix result[5] ($\nu\simeq0.82$ for $\kappa=0.4$ and $\alpha=0.36$ from the scaling relationship $d\nu=2-\alpha$) from which one obtains $\alpha/\nu\simeq0.44$. However, we cannot find arguments to support the existence of a nonuniversal F-P transition line with critical exponents that change continuously as function of κ. In our opinion this contrasts with the universality hypothesis: indeed for $0<\kappa<1/2$ the ground state of the ANNNI model is F and the symmetry of the Hamiltonian does not change. Moreover the presence of a Lifshitz point on the F-P transition line is definitively ruled out.[3] For this reason we are in favor of the first hypothesis of Grynberg and Ceva[5] according to which the ANNNI model has a Ising-type behavior for any $0<\kappa<1/2$.

To check the effect of a rectangle-shaped sample we have performed simulations on lattice 96×12 and 12×96 where the second number refers to the number of spins in the axial direction. The first choice leads to a specific heat very close to that obtained for a square lattice 96×96 [see (magenta) open squares in Fig. 1(b)] and similar to that shown in Fig. 2 of Grynberg and Ceva[10] for $\kappa=0.45$ obtained from a transfer-matrix calculation with $N=12$. The second choice [see (blue) open circles in Fig. 1(b)] leads to a specific heat similar to that obtained for $\alpha=0.285$ in Fig. 4 of Selke[9] except for the absence of the (spurious) low-temperature peak. The lesson to be learned from this result is that the rectangular lattice can compete with the square one only if the *short* side of the rectangle is chosen to coincide with the axial direction where competition is present. Incidentally, this is the basic assumption in any transfer-matrix calculation where lattices $\infty\times L$ are considered. Anyway the use of rectangle-shaped lattices is unfavorable for $\kappa>1/2$ since the short side along the axial direction implies a very restricted number of wave vectors. For instance the maximum number of L in a transfer-matrix calculation[5] is 12 so that the only eligible wave vectors are $\pi/2$, $\pi/3$ and $\pi/6$ not many to investigate the IC phase. In conclusion we think that the best choice is a $L\times L$ square lattice.

The transition temperature $T_f(\kappa)$ between the F and P phases obtained from MC simulation is in good agreement with the FFA result[3]

$$\frac{k_BT_f}{J}\exp\left(-\frac{2J}{k_BT_f}\right)=1-2\kappa \tag{8}$$

as shown in Fig. 14 comparing full circles (MC) with the continuous curve.

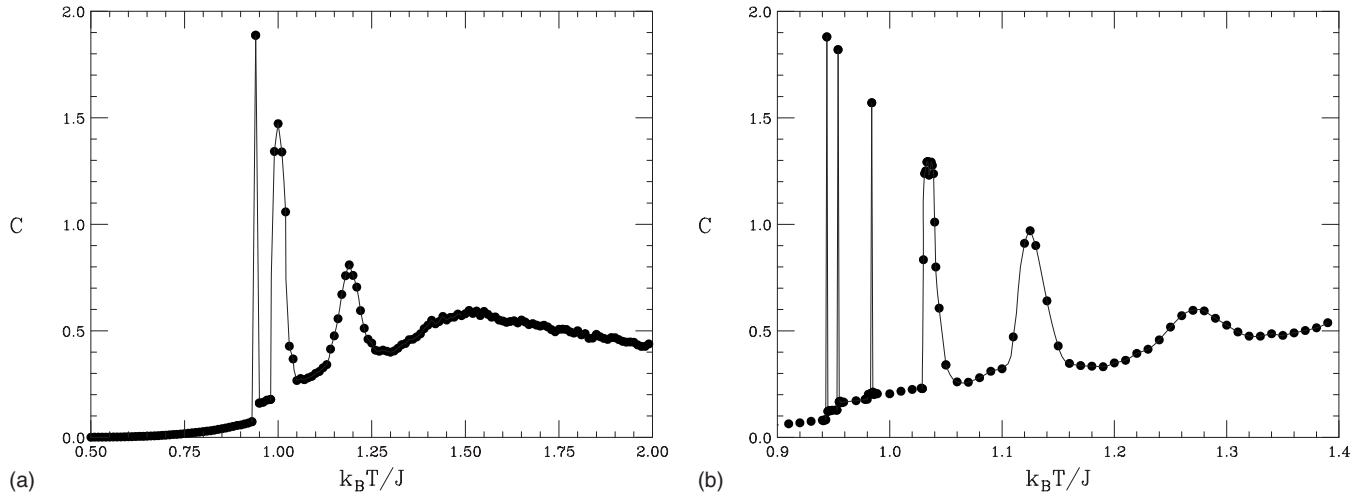

FIG. 2. Specific heat vs temperature for $\kappa=0.6$ obtained from a simulation of 10^7 MCS for lattices of side (a) $L=48$ and (b) $L=96$.

Unexpected results are obtained for $\kappa>1/2$. The specific heat vs temperature shows a multipeak structure for $\kappa=0.6$, $L=48$ and 96 as shown in Fig. 2. Each peak corresponds to a discontinuous change of the q wave vector accompanied by a discontinuous change in the energy. A sort of complete devil's staircase is obtained because of the discreteness of the lattice. In Fig. 2(a) the peaks correspond to the steps of q from $\pi/2$ to $11\pi/24$, from $11\pi/24$ to $10\pi/24$, and from $10\pi/24$ to $9\pi/24$, respectively. Analogously the peaks in Fig. 2(b) correspond to change of q from $\pi/2$ to $23\pi/48$, $22\pi/48$, $21\pi/48$, $20\pi/48$, and $19\pi/48$. This scenario is supported by the calculation of the structure factor

$$S(0,q)=\left\langle \frac{|\sigma(0,q)|^2}{L^2}\right\rangle, \quad \sigma(0,q)=\frac{1}{L}\sum_{m,n} S_{m,n}e^{iqn} \qquad (9)$$

where m runs over the L sites of a row and n over the L sites of a column (axial direction). As it is well known $S(\boldsymbol{q})$ is related to the kind of order ($\boldsymbol{q}$) and to the amount of order (magnitude). As shown in Fig. 3 the kind of order changes

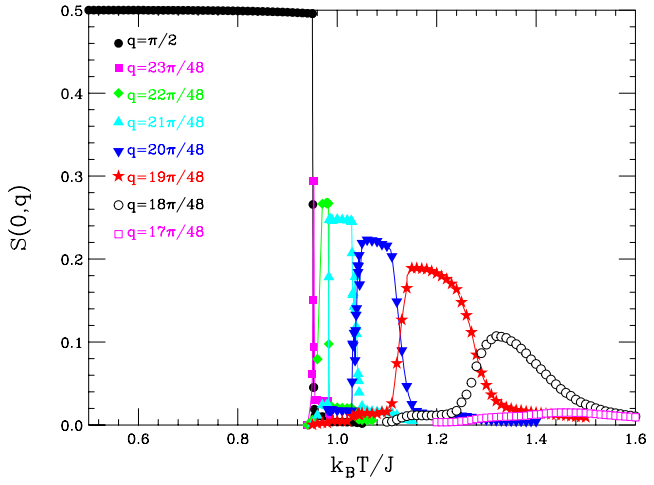

FIG. 3. (Color online) Structure factor intensity vs temperature for several values of the wave vector for a lattice of side $L=96$ as obtained from a simulation of 10^7 MCS.

abruptly at any change in the wave vector $\boldsymbol{q}=(0,q)$ where $q=2\pi n/L$ with $n=L/4, L/4-1, \ldots$. The steep changes occurring at the first steps lead to believe that it is very hard to find the coexistence between the two states with neighbor wave vectors. The meaning of the third and fourth peaks in the specific heat of Fig. 2(b) is well understood looking at the energy-time series that shows the coexistence of the phases corresponding to $q=22\pi/48$ (E_2) and $q=21\pi/48$ (E_3) for $k_BT/J=0.984$ [Fig. 4(a)] and the coexistence of phases corresponding to $q=21\pi/48$ (E_3) and $q=20\pi/48$ (E_4) for $k_BT/J=1.04$ [Fig. 4(b)]. Note that in the first case a temperature step of $k_B\Delta T/J=0.001$ was required to find the coexistence between the states E_2 and E_3. We were not able to find analogous time series for the first two peaks. Only one jump in the energy from the lower-temperature phase to the higher temperature one was recorded. In four independent runs of 10^7 MCS rising the temperature by a step of $\Delta k_BT/J=0.01$ we found that the first peak of the specific heat corresponding to the jump $E_0\rightarrow E_1$ occurred at $k_BT/J=0.94$ (one run) or at 0.95 (three runs). The second peak corresponding to the jump $E_1\rightarrow E_2$ occurred at $k_BT/J=0.95$ (one run), at 0.96 (two runs), and at 0.97 (one run). The location of the first peak was confirmed looking at energy-time series of simulations of 10^8 MCS for $k_BT/J=0.942, 0.944, 0.946, 0.948$. Each simulation was performed starting from the ground-state configuration $\langle 2\rangle$. All these simulations showed the transition $E_0\rightarrow E_1$ with $\frac{E_1-E_0}{JL^2}=0.027$. No jump was found for $k_BT/J=0.940$ (E_0) or 0.950 (E_1) so that the incertitude of the transition temperature between the $\langle 2\rangle$ and the IC phase is within $k_B\Delta T_a/J\simeq 0.005$.

The difficulty of observing the coexistence (several steps upward and downward in the energy-time series) is due to the very long relaxation time between the coexisting phases, greater than 10^8 MCS. In order to draw the first two peaks of the specific heat we assume that the transition between the phases E_s and E_{s+1} are discontinuous as clearly shown by the jump in the energy-time series so that the maximum of the specific heat is given by[11]

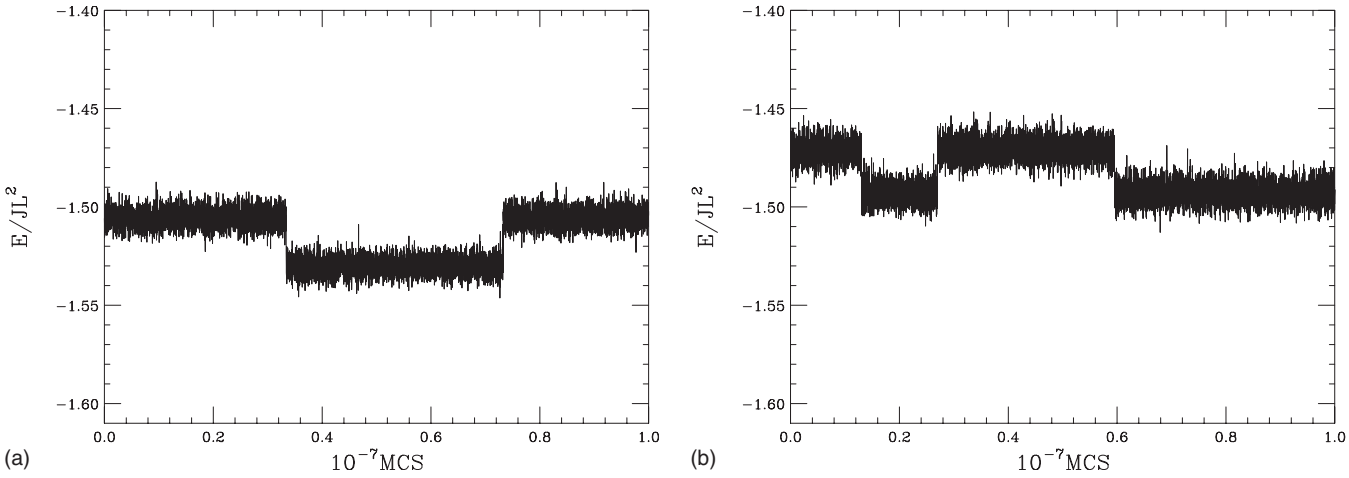

FIG. 4. Energy-time series for a lattice of side $L=96$ and $\kappa=0.6$: (a) $k_BT/J=0.984$ and (b) $k_BT/J=1.04$.

$$C_L^{\max}=\left[\frac{1}{2}\left(\frac{E_{s+1}-E_s}{JL^2}\right)\left(\frac{J}{k_BT}\right)L\right]^2. \tag{10}$$

We tested the reliability of this formula for the jumps $E_2 \rightarrow E_3$ and $E_3 \rightarrow E_4$ where the coexistence was proved by the energy time series as shown in Fig. 4. The crucial difference between a first-order phase transition and the $\langle 2\rangle$-IC transition is that in the latter $\frac{\Delta E}{JL^2}=\frac{E_1-E_0}{JL^2}$ is not independent of L but reduces by a factor 2 when L is doubled (for instance $\frac{\Delta E}{JL^2}=0.027$ for $L=96$ and 0.054 for $L=48$). The fact that $\frac{\Delta E}{JL^2}\times L$ is nearly constant and the temperature of the first jump is nearly independent of L ($k_BT_a/J\simeq 0.94$ for $L=24$, 48, and 96) implies that the height of the specific-heat peak obtained from Eq. (10) is about 1.9 independent of the lattice size as shown in Figs. 2(a) and 2(b).

The specific heat of Fig. 2 differs from both the specific heat shown in Fig. 5 of Selke[9] and that shown in Fig. 4 of Sato and Matsubara[12] who performed an MC simulation on lattices $L\times 2L$ (with $L=16,24,32,48,64$) using an algorithm called cluster heat bath method which, updating clusters of spins instead of a single spin, enables the authors to reduce the equilibration time of more than one order of magnitude with respect to the conventional importance sampling Monte Carlo method.[13] The specific heat of Refs. 9 and 12 shows a two-peak structure: a sharp peak at lower temperature and a broad one at higher temperature. The large error bars around the sharp peak shown in Fig. 4 of Ref. 12 indicate that the system did not reach the thermal equilibrium. We try to overcome the failure of equilibrium looking at the time series of the energy and making use of Eq. (10) to evaluate the maximum of the specific heat occurring at any change in the wave vector.

We find very good agreement between our transition temperature $T_a(\kappa)$ between the $\langle 2\rangle$ and the IC phase and that obtained by the FFA (Ref. 3)

$$2\frac{k_BT_a}{J}\exp\left(-\frac{2J}{k_BT_a}\right)=2\kappa-1. \tag{11}$$

This surprising good agreement is justified by looking at the snapshots given in Fig. 5. The pictures illustrate as Villain and Bak[3] captured the essence of the IC phase where defected three-walls domains are the main excitations that destroy the long-range order of the $\langle 2\rangle$ phase. As one can see going from (a) (up left) to (d) (down right) 4, 8, 12 and 16 three-wall domains can be recognized. Approaching the transition temperature between the IC and the P phase some bound dislocations appear in agreement with Fig. 4 of Ref. 1. This kind of excitation (the presence of a number of three-wall domains multiple of 4 with density $\langle w\rangle/L=4s/L$) changes discontinuously either the wave vector $q=\frac{\pi}{2}(1-4s/L)$ and the energy E_s in a finite lattice leading to the sharp peaks in the specific heat. At higher temperature new excitations appear such as unbound dislocations that broaden the specific-heat peaks.

A problem arises out of the assignment of the critical temperature T_c of the IC-P phase transition. We take advantage from the high-temperature series (HTS) expansion of the wave-vector-dependent susceptibility[14] $\chi(q)=S(0,q)L^2$ that leads to Fig. 5 of Ref. 14 when the Padé approximant method is used. We checked that this temperature is close to the temperature of the last maximum of the specific heat of our simulations with $L=96$. For $\kappa=0.6$, 0.8, 1, 1.5, and 2 we find that the last maximum of the specific heat occurs at $k_BT_c/J\simeq 1.27$, 1.70, 1.98, 2.60, and 3.23, respectively, to be compared with the corresponding HTS result $k_BT_c/J=1.21$, 1.73, 2.05, 2.68, and 3.25.

The crucial role played by the lattice size and consequently the discreteness of the wave vector is well shown in Figs. 6 and 7 where the specific heat, internal energy, and structure factor vs temperature are quoted for $L=24,48,96$. In Fig. 6 one sees that the number of peaks in the specific heat increases when the lattice size increases. The temperature corresponding to the $\langle 2\rangle$-IC phase transition is $k_BT_a/J\simeq 1.36$ for both $L=48$ and 96. Also the number of energy jumps increases with L even though their magnitude is halved.

For $\kappa=0.8$ the wave vector at the IC-P transition is $q=5\pi/12$ for $L=24$ and 48, a mixing of $q=21\pi/48$ and $20\pi/48$ for $L=96$ to be compared with the HTS result[14] $q\simeq 0.41\pi$. The agreement is better as the lattice size increases, as one expects on the basis of the increasing number of avail-

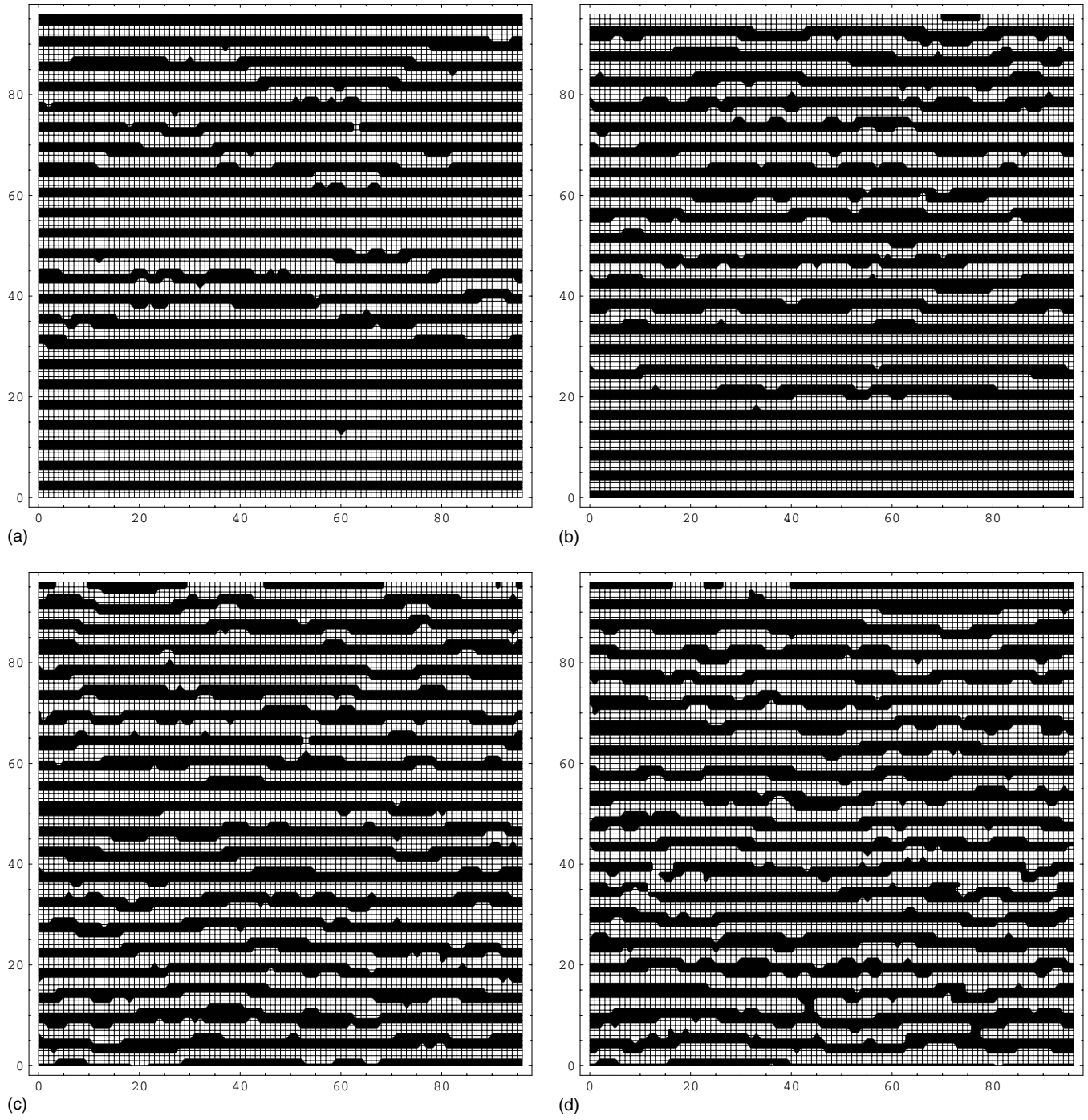

FIG. 5. Snapshots for a lattice of side $L=96$ and $\kappa=0.6$ for (a) $k_BT/J=0.95$, (b) $k_BT/J=0.96$, (c) $k_BT/J=1.03$, and (d) $k_BT/J=1.06$.

able wave vectors. For $L=24$ only one incommensurate wave vector is selected in the IC phase; two for $L=48$, and three and four for $L=96$. This is a pure effect of the finite lattice size.

The structure factor shown in Fig. 7 for $L=24$, 48, and 96 enlights the nature of the IC phase characterized by a complete devil's staircase of the wave vector: all wave vectors consistent with the lattice size in the range between $\pi/2$ and[14] $q_\infty=\arccos(\frac{1}{4\kappa})$ are spanned. It is interesting to notice the different behaviors of the magnitude of the structure factor in the ordered $\langle 2\rangle$ phase and in the KT-like IC phase. Indeed in the $\langle 2\rangle$ phase the structure factor is about 1/2 for any lattice size as shown by the (black) full circles of Fig. 7 whereas in the IC phase a clear size dependence is seen looking at the data points corresponding to $q=5\pi/12$ (blue downward triangles for $L=24$, 48, and 96) or $q=11\pi/24$ (green diamonds for $L=48$ and 96). The scaling toward zero is a clue of the absence of long-range order in the IC phase as expected.[3]

The specific heat vs temperature for $L=24,48,96$ and the structure factor for $L=96$ are quoted in Figs. 8–10 for $\kappa=1,1.5,2$, respectively. For all κ's the lattice with $L=24$

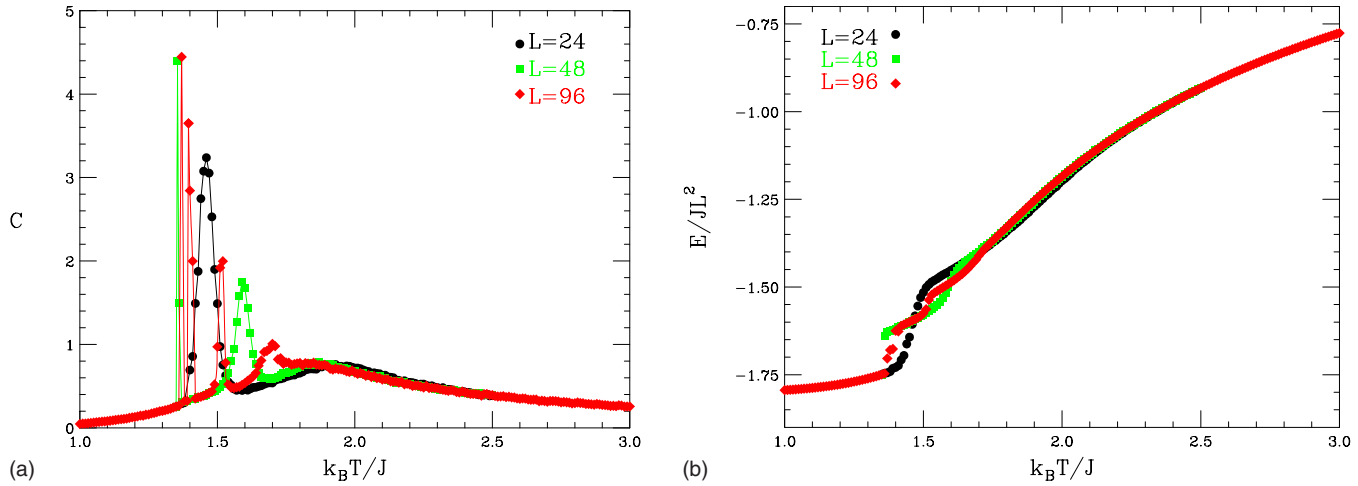

FIG. 6. (Color online) (a) Specific heat and (b) energy vs temperature for $\kappa=0.8$ for lattice of several sides: $L=24$ (full circles), $L=48$ (green squares), and $L=96$ (red diamonds).

shows a single peak in the specific heat pointing out the existence of a single phase transition between the $\langle 2 \rangle$ and the P phase. For $\kappa=1.5$ and 2 the same occurs for a lattice with $L=48$ while a double transition survives up to $\kappa=2$ for $L=96$. Notice the remarkable resemblance between Fig. 10(b) (structure factor for $\kappa=2$ and $L=96$) and Fig. 7(a) ($\kappa=0.6$ and $L=24$). This means that increasing κ further also the specific heat of the lattice with $L=96$ will show a single peak

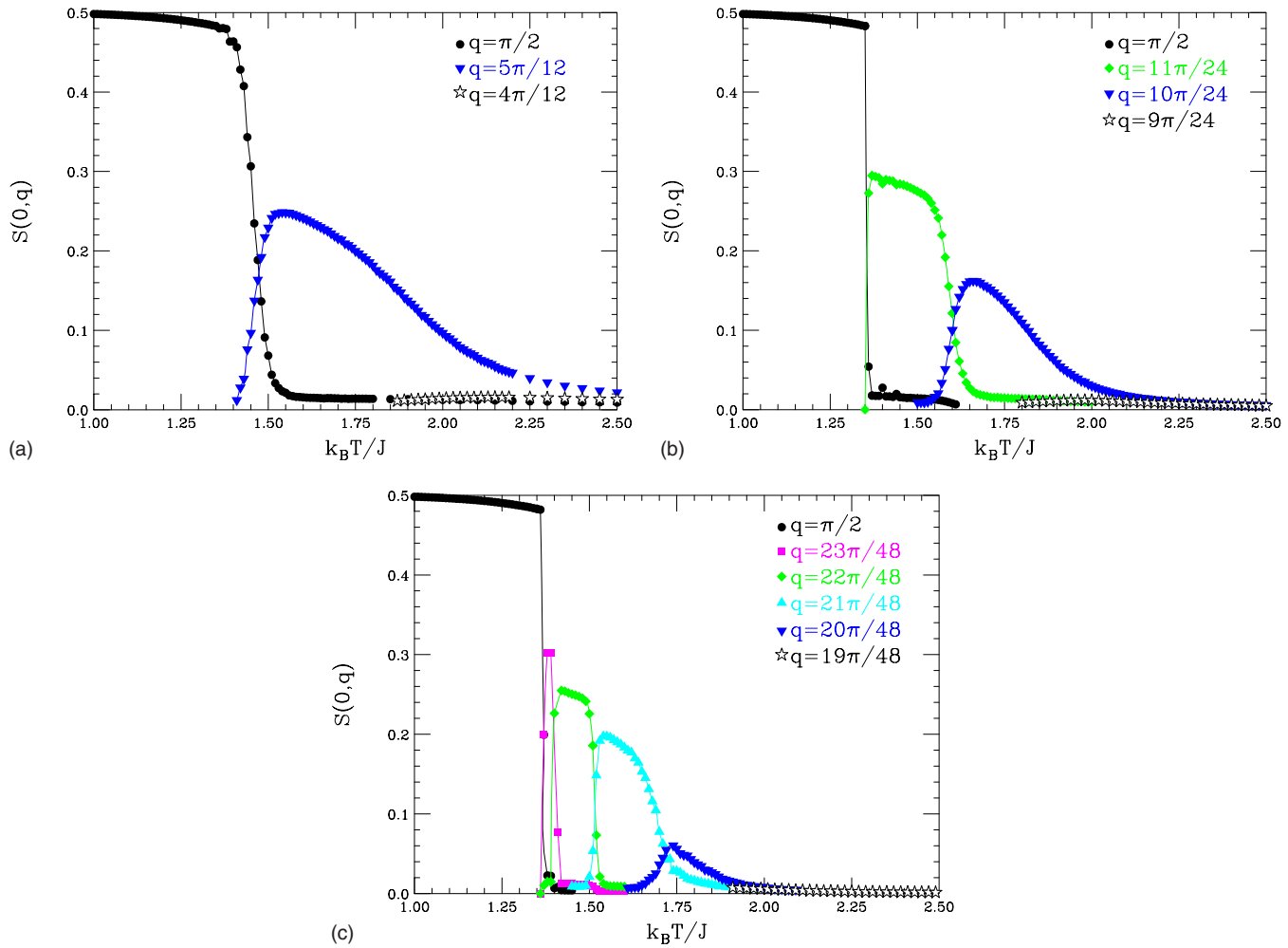

FIG. 7. (Color online) Structure factor intensity vs temperature for $\kappa=0.8$ and several values of the wave vector for a lattice of side (a) $L=24$, (b) $L=48$, and (c) $L=96$.

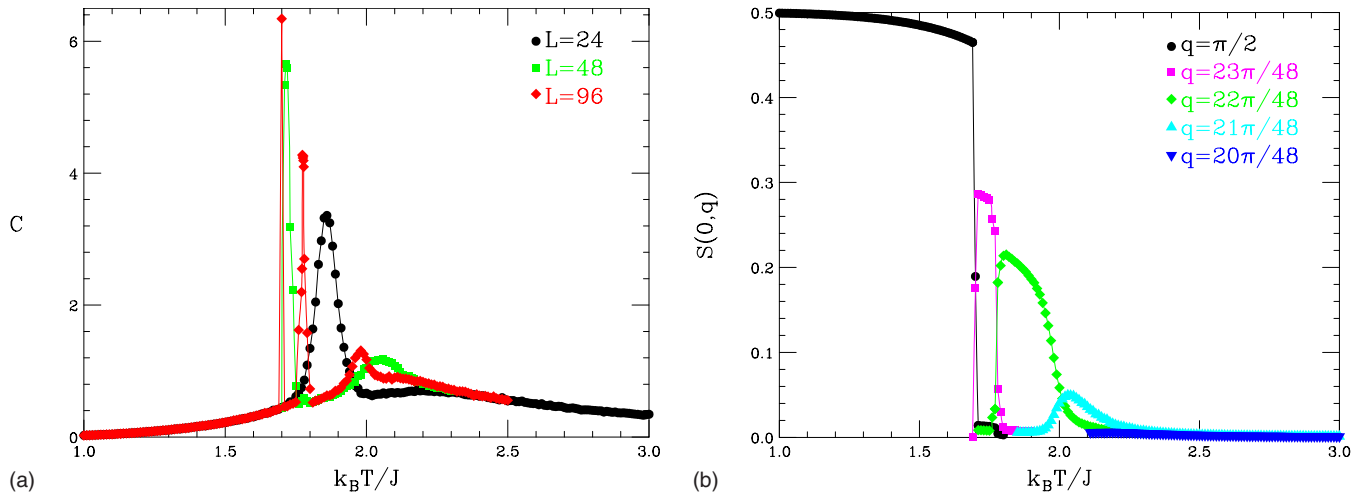

FIG. 8. (Color online) (a) Specific heat for lattices of several sides and (b) structure factor intensity for $L=96$ vs temperature for $\kappa=1$ and 10^7 MCS.

leading to a single transition between the $\langle 2\rangle$ and the P phase as confirmed by Fig. 11 where the specific heat and structure factor for a lattice size $L=96$ and $\kappa=3$ is shown. The disappearance of all peaks except one in the specific heat might support the existence of a Lifshitz point along the $\langle 2\rangle$-P transition line. In particular, one finds that κ_L is about 0.8, 1.5, and 3 for $L=24$, 48, and 96, respectively. However, we think that this conclusion is only a direct consequence of the finite size of the lattice. Indeed κ_L increases with L in a nearly linear way so that we conclude that the Lifshitz point goes to infinity in the thermodynamic limit.

In Fig. 12 we give the energy-time series for $\kappa=2$, $L=96$, and $k_BT/J=2.93$, the temperature corresponding to sharp peak in the specific heat of Fig. 10(a). As one can see the coexistence of the $\langle 2\rangle$ and the IC phase with $q=23\pi/48$ is clearly seen. Only for temperatures $k_BT/J\gtrsim 2$ the relaxation time is short enough ($<10^7$) to see the coexistence of the ordered and modulated phase over an accessible computer time. When κ decreases the coexistence occurs at lower temperatures and the relaxation time becomes quickly greater than any accessible computer time so that we use Eq. (10) to obtain the height of the first peak for $\kappa\lesssim 2$.

In Fig. 13 we show the complete devil's staircase for the order wave vector q/π vs temperature for $L=96$ and $\kappa=0.6, 0.8, 1, 1.5, 2$. In the thermodynamic limit these devil's staircases are expected to become continuous curves of the temperature.

Finally, in Fig. 14 we give the phase diagram of the ANNNI model on a lattice of size $L=96$ that should be very close to that one expects in the thermodynamic limit. For comparison continuous lines corresponding to the FFA (Ref. 3) are drawn.

An open question concerns the shape of the specific heat in the thermodynamic limit: what happens to the several sharp peaks appearing in the specific heat as a direct consequence of the finite lattice size? Finite-size scaling seems to point out that for the first peak of the specific heat corresponding to the transition from the $\langle 2\rangle$ to the IC phase with four three-wall domains, Eq. (10) is satisfied assuming $(E_1-E_0)\propto JL$ (instead of JL^2 as for a first-order phase transition)

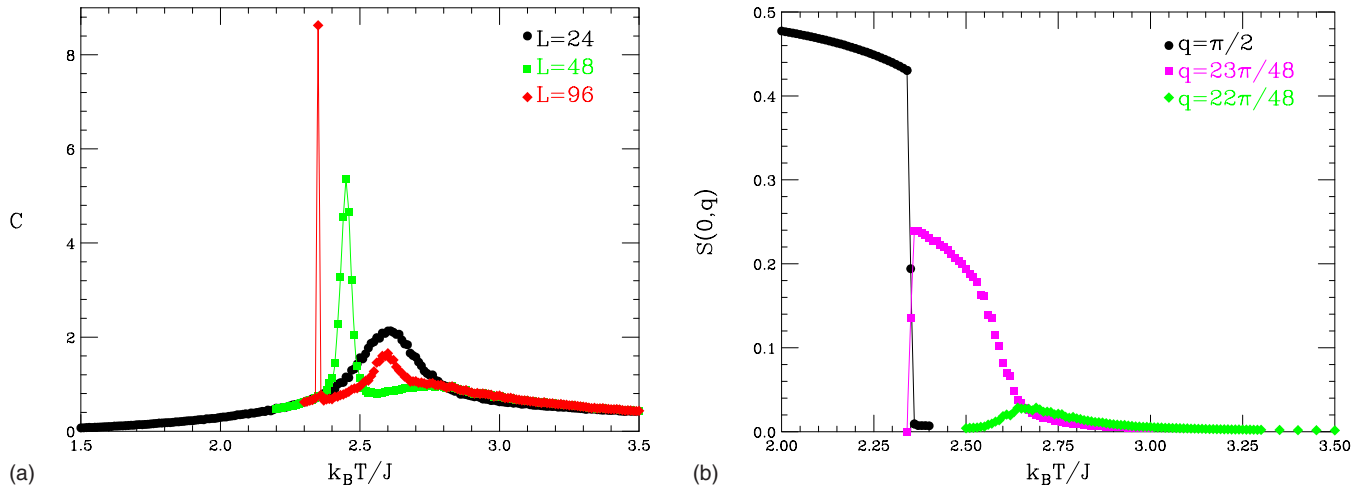

FIG. 9. (Color online) (a) Specific heat for lattices of several sides and (b) structure factor intensity for $L=96$ vs temperature for $\kappa=1.5$ and 10^7 MCS.

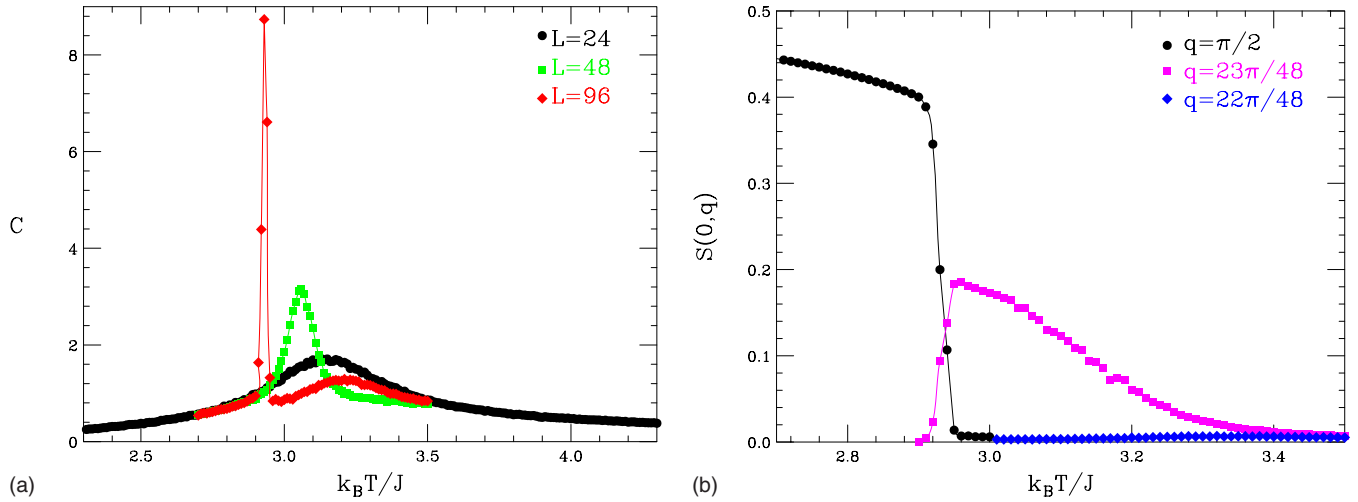

FIG. 10. (Color online) (a) Specific heat for lattice of several sides and (b) structure factor intensity for $L=96$ vs temperature for $\kappa=2$ and 10^7 MCS.

leading to a discontinuity in the specific heat similar to that observed in the Stanley model,[15] a two-dimensional Ising model where each spin interacts equally with all other spins of the lattice by a ferromagnetic exchange coupling $2J/L^2$. This model gives exactly the mean-field critical exponents: in particular, the specific heat is $C/(k_BL^2)=\frac{3}{2}-\frac{12}{5}\frac{T_c-T}{T_c}$ for $T\to T_c^-$ and $C/(k_BL^2)=0$ for $T>T_c$. The discontinuity $\Delta C/(k_BL^2)=3/2$ at the critical temperature $k_BT_c/(2J)=1$ is clearly seen performing MC simulation on such a model: we find that the maximum of the specific heat does not scale with L as expected. On the contrary the existence of a cusp in the internal energy at the transition is not easy to point out by MC simulations. The absence of scaling found in the first peak of the specific heat of the ANNNI model for $\kappa>1/2$ seems to indicate a discontinuity in the specific heat at the transition between the $\langle 2\rangle$ and the IC phase instead of the well-established logarithmic divergence observed for $\kappa<1/2$. Notice that only an unobservable essential singularity in the specific heat is expected in a genuine KT transition.[16]

It is worthwhile noticing that the FFA (Ref. 3) provides the following specific heat:

$$C/(k_BL^2)=\left(\frac{J}{k_BT}\right)^2\left[\frac{8}{\pi}\exp\left(-\frac{2J}{k_BT}\right)(1-\rho)\sin\frac{\pi\rho}{1-\rho}\right.$$
$$\left.+\frac{2}{\pi}(1-2\kappa)^2\left(1+2\frac{J}{k_BT}\right)^2\exp\left(\frac{2J}{k_BT}\right)\frac{(1-\rho)^3}{\sin\frac{\pi\rho}{1-\rho}}\right], \quad (12)$$

where ρ is the density of walls given by the equation

$$\frac{1}{1-\rho}\cos\frac{\pi\rho}{1-\rho}-\frac{1}{\pi}\sin\frac{\pi\rho}{1-\rho}=\frac{J}{k_BT}(1-2\kappa)\exp\left(\frac{2J}{k_BT}\right) \quad (13)$$

ρ is 0 or 1/2 in the F or $\langle 2\rangle$ phase, respectively. For $T\to T_f$ one has

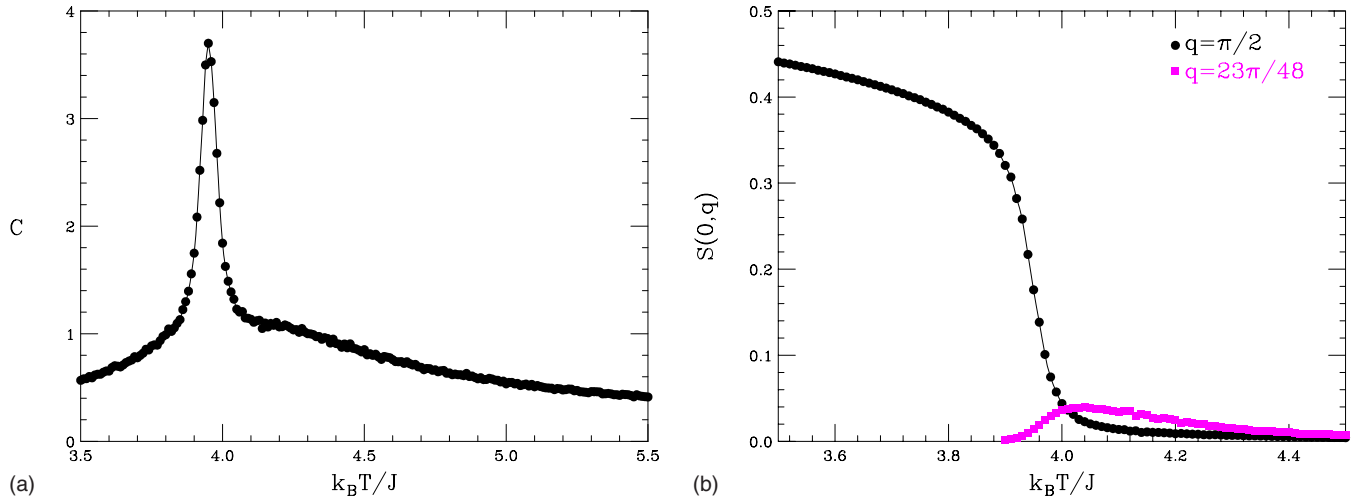

FIG. 11. (Color online) (a) Specific heat and (b) structure factor intensity vs temperature for a lattice of side $L=96$, $\kappa=3$, and 10^7 MCS.

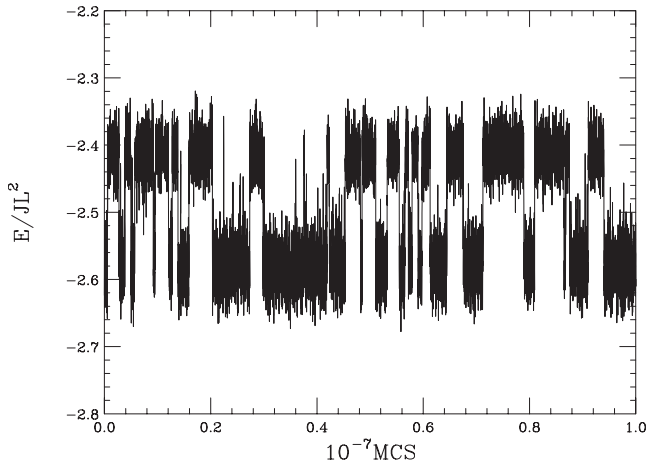

FIG. 12. Energy-time series for $\kappa=2$ and $k_BT/J=2.93$ for a lattice of side $L=96$.

$$\rho = \frac{\left(4+2\frac{k_BT_f}{J}\right)^{1/2}}{\pi\frac{k_BT_f}{J}}\left[\frac{k_B}{J}(T-T_f)\right]^{1/2} + O(T-T_f) \quad (14)$$

and

$$C/(k_BL^2) = \frac{2\pi\left(1+2\frac{J}{k_BT_f}\right)^2\frac{k_BT_f}{J}\exp\left(-\frac{2J}{k_BT_f}\right)}{\left(4+2\frac{k_BT_f}{J}\right)^{1/2}} \times\left[\frac{k_B}{J}(T-T_f)\right]^{-1/2} + 8\left(\frac{J}{k_BT_f}\right)^2\exp\left(-\frac{2J}{k_BT_f}\right) - \frac{16}{3}\left(1+\frac{2J}{k_BT_f}\right)^2\exp\left(\frac{2J}{k_BT_f}\right) + O[(T-T_f)^{1/2}], \quad (15)$$

where T_f is obtained from Eq. (8). For $T\to T_a$ one has

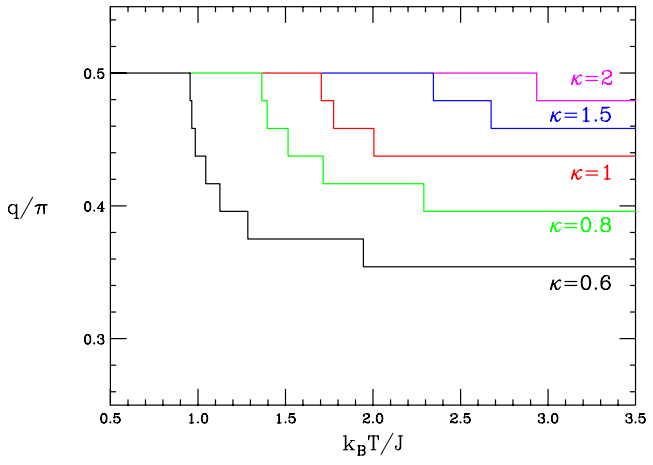

FIG. 13. (Color online) Wave vector (in units of π versus temperature for several κ as obtained from MC simulations on a lattice of side $L=96$.

$$\rho = \frac{1}{2} - \frac{\left(4+2\frac{k_BT_a}{J}\right)^{1/2}}{4\pi\frac{k_BT_a}{J}}\left[\frac{k_B}{J}(T-T_a)\right]^{1/2} + O(T-T_a), \quad (16)$$

$$C/(k_BL^2) = \frac{\left(1+2\frac{J}{k_BT_a}\right)^2\frac{k_BT_a}{J}\exp\left(-\frac{2J}{k_BT_a}\right)}{\pi\left(4+2\frac{k_BT_a}{J}\right)^{1/2}}\left[\frac{k_B}{J}(T-T_a)\right]^{-1/2} + \frac{4}{3\pi^2}\left(1+2\frac{J}{k_BT_a}\right)^2\exp\left(-\frac{2J}{k_BT_a}\right) + O[(T-T_a)^{1/2}], \quad (17)$$

where T_a is obtained from Eq. (11).

As one can see the wave vector $q=\pi\rho$ goes to zero ($\kappa<1/2$) or to $\pi/2$ ($\kappa>1/2$) as a square root of $T-T_f$ or $T-T_a$, respectively. For $\kappa>1/2$ the square-root behavior is in qualitative agreement with the temperature dependence of the wave vector shown in Fig. 13. For $\kappa=0.6$ Sato and Matsubara[12] find a density of three walls that goes to zero as $\langle w\rangle/L=(1/2-\rho)\sim(T-T_a)^\beta$ with $\beta=1/2$ and a correlation length ξ that diverges as $\xi\sim(T-T_a)^{-\nu}$ with $\nu=1$. The temperature dependence of the density of three-walls domains is in agreement with Eq. (16) that gives $\langle w\rangle/L=0.2116[(k_BT/J)-0.9070]^{1/2}$ for $\kappa=0.6$. The power-law behavior of the correlation length, however, is unexpected for a conventional KT phase where the divergence of the correlation length is predicted over the whole region of existence of the KT phase ($T_a<T<T_c$). On the other hand the divergence of the FFA specific heat as $0.1356(k_BT/J-0.9070)^{-1/2}+0.1530$ for $T\to T_a^+=0.9070J/k_B$ confirms that the IC phase is a sui generis KT phase. On the contrary our numerical simulations seem to point out a discontinuity ($\alpha=0$) in the specific heat at T_a rather than a divergence. This hypothesis is compatible with the result of Sato and Matsubara[12] ($\nu=1$) since the scaling relation $d\nu=2-\alpha$ is satisfied.

III. SUMMARY AND CONCLUSIONS

We have studied the 2D ANNNI model by Monte Carlo simulation in order to better understand the nature of the F-P, the $\langle 2\rangle$-IC, and the IC-P phase transitions. The phase diagram of the model in the plane ($\kappa=-J_2/J$ and k_BT/J) is shown in Fig. 14. The Ising nature of the F-P phase transition for $\kappa<1/2$ is supported by the logarithmic scaling with size of the specific heat maximum in agreement with the exact result[8] obtained for a pure NN Ising model. The specific heat for $\kappa>1/2$ shows a multipeak profile never emphasized in previous analysis. Certainly this is an artifact of the finite size $L\times L$ of the lattice that implies a discrete number of wave vectors $q=2\pi n/L$: this size dependence is clearly seen looking at the number of peaks in the specific heat that increases as L increases. Anyway the location and the height of first peak of the series corresponding to the $\langle 2\rangle$-IC phase transition seem to be independent of the size. We think that

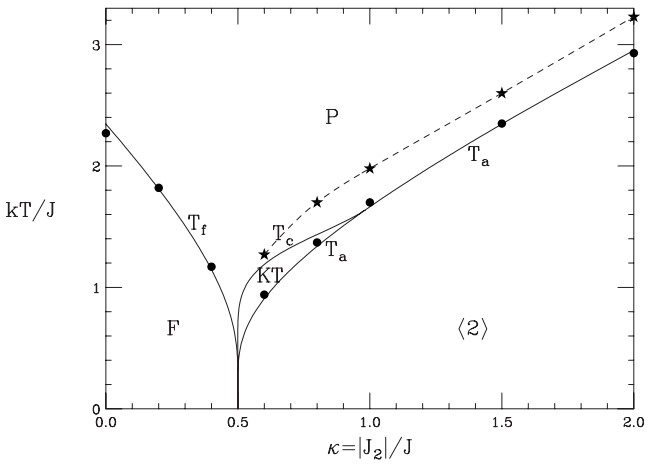

FIG. 14. Phase diagram of the ANNNI model: continuous curves obtained from Ref. 3. Full circle and stars obtained from MC simulations on a lattice of side $L=96$.

such a behavior is consistent with the existence of a cusp in the internal energy and a discontinuity in the specific heat at the $\langle 2\rangle$-IC transition when the thermodynamic limit is performed.

The snapshots taken during the energy-time series at several temperatures support the occurrence of four three-wall domains consisting of three rows of spins up or down at the $\langle 2\rangle$-IC transition in agreement with the free fermion approximation.[3] At increasing temperature eight, 12, and 16 three-wall domains can be recognized from the snapshots at $\kappa=0.6$. The apparent shrinking of the IC phase at increasing κ might erroneously suggest the existence of a Lifshitz point along the $\langle 2\rangle$-P boundary. However, we think that this is not the case since we have checked that increasing the lattice size the Lifshitz point is pushed to larger κ so that we think that the Lifshitz point reaches the infinity for $\kappa\to\infty$.

The size scaling of the structure factor $S(0,q)$ supports the common expectation that the modulated phase is of KT nature. Indeed we find that $S(0,\frac{\pi}{2})$ is independent of the size in the (ordered) $\langle 2\rangle$ phase whereas $S(0,q)$ becomes lower and lower in the IC phase as L increases as shown in Figs. 8 and 9. Moreover the structure factor remains δ-like shaped in the IC phase. The peak in $S(0,q)$ which cannot be a rigorous $\delta(q)$ function because the IC phase does not have long-range order, is expected to move continuously with q in the thermodynamic limit where the wave vector q becomes a continuous function of the temperature. Only at the IC-P transition the peak broadens and loses intensity.

As it is well known MC simulations are difficult in anisotropic systems where the relaxation time may be very large. Very long simulations give us confidence on the most of the data. Only for $\kappa\to 1/2$ we were not able to reach equilibrium as for the first peak in the specific heat. However, taking advantage of the empirical relationship between the jump in energy and the height of the peak in the specific heat,[11] we think that all peaks of the specific heat for $\kappa=0.6$ could be reliable.

The problem is to catch the evolution of the specific heat in the thermodynamic limit. We have proved that the peaks become more frequent as L increase since an increasing number of wave vectors are available so that one could expect that an envelope of those peaks might occur for $L\to\infty$. The last peak, on the contrary, which is not related to a change in a single wave vector but rather to a superposition of several wave vectors is the sign of a genuine IC-P transition. As for the $\langle 2\rangle$-IC we think of a second-order phase transition characterized by a discontinuity in the specific heat instead of a divergence as given by the free fermion approximation.

We have also checked that the choice of a square lattice is better than a rectangular one. This latter choice gives good results when the (short) side is chosen to coincide with the axial direction in agreement with the results obtained by the transfer matrix method where samples of $\infty\times L$ are investigated, assuming L in the axial direction.[5] On the contrary we find a very slow convergence when the short side of the rectangle is chosen perpendicular to the axial direction. In any case the transfer matrix method is severely influenced by the very small number of available wave vectors for $\kappa>1/2$ since the actual calculation is inhibited by the quick increasing in the transfer matrix dimension $2^L\times 2^L$ that prevents any calculation for $L\gtrsim 12$.

*Present address: Istituto IMEM of CNR, Parco Area delle Scienze, 43100 Parma, Italy; rastelli@fis.unipr.it

[1] W. Selke, Phys. Rep. **170**, 213 (1988).
[2] J. Stephenson, Can. J. Phys. **48**, 1724 (1970).
[3] J. Villain and P. Bak, J. Phys. (France) **42**, 657 (1981).
[4] D. A. Huse and M. E. Fisher, J. Phys. C **15**, L585 (1982).
[5] M. D. Grynberg and H. Ceva, Phys. Rev. B **38**, 9172 (1988).
[6] T. Garel and P. Pfeuty, J. Phys. C **9**, L245 (1976).
[7] L. Onsager, Phys. Rev. **65**, 117 (1944).
[8] A. E. Ferdinand and M. E. Fisher, Phys. Rev. **185**, 832 (1969).
[9] W. Selke, Z. Phys. B: Condens. Matter **43**, 335 (1981).
[10] M. D. Grynberg and H. Ceva, Phys. Rev. B **36**, 7091 (1987).
[11] M. S. S. Challa, D. P. Landau, and K. Binder, Phys. Rev. B **34**, 1841 (1986).
[12] A. Sato and F. Matsubara, Phys. Rev. B **60**, 10316 (1999).
[13] L. P. Landau and K. Binder, *A Guide to Monte Carlo Simulations in Statistical Physics* (Cambridge University Press, Cambridge, 2005).
[14] J. Oitmaa, J. Phys. A **18**, 365 (1985).
[15] H. E. Stanley, *Introduction to Phase Transitions and Critical Phenomena* (Oxford University Press, Oxford, 1971).
[16] D. R. Nelson, in *Phase Transitions and Critical Phenomena*, edited by C. Domb and J. L. Lebowitz (Academic Press, London, 1983), Vol. 7.